J. Acoust. Soc. Jpn. (*E*) **17**, 6 (1996)

Optimal on-line modeling of primary and secondary paths in active noise control systems

Nozomu Saito,* Toshio Sone,* Tomohiko Ise,** and Masaichi Akiho**

**Research Institute of Electrical Communication/*
Graduate School of Information Sciences, Tohoku University,
2-1-1, Katahira, Aoba-ku, Sendai, 980-77 Japan
***Alpine Electronics, Inc.,*
20-1, Yoshima, Kogyodanchi, Iwaki, 970-11 Japan

(*Received 18 December 1995*)

The modeling error shown by the difference of the characteristics between the secondary paths and its models will cause the improper adaptation of the filtered-x LMS adaptive filters in active noise control systems. It is necessary to use the on-line modeling systems for avoiding such improper adaptation, and several on-line modeling methods have been proposed hitherto. Especially, one of them is very useful because the method can identify the primary and the secondary path characteristics without using any additional signal. This method, however, will not always provide the proper modeling results, and the conditions for optimizing the results have not been discussed yet. This paper investigates the conditions for optimal on-line modeling of the primary and the secondary path characteristics without using any additional signal for identification. Theoretical analysis produces the specific conditions which the noise control adaptive filter should satisfy. Those results of the theoretical consideration are confirmed by the computer simulation in which the impulse responses measured in a vehicle cabin are used.

Keywords: Active noise control, Filtered-x LMS algorithm, Modeling error, On-line modeling, Interior car noise

PACS number: 43. 50. Ki

1. INTRODUCTION

The filtered-x LMS (Least Mean Square) algorithm[1,2] has been applied to many practical cases in active noise control. This algorithm has the simple structure and shows the relatively good performance. Therefore, the filtered-x LMS algorithm is very useful in most of the engineering problems, even though the algorithm has tight limitation. This algorithm contains the transfer function model of the secondary path, which has the acoustical transfer function between the output of the noise control adaptive filter and the output of the error sensor. Thus, the performance of the algorithm would inevitably be influenced by accuracy of the transfer function model of the secondary path. The difference between the correct transfer function of the secondary path and their model, that is called modeling error, will cause the improper adaptation. In other words, the noise control adaptive filter cannot update itself correctly due to modeling error that originates from any sources.[3-6]

We can avoid such improper adaptation caused by modeling error using on-line modeling techniques. Several on-line modeling methods have been proposed in the last decade.[7-10] In those proposals, there are basically two approaches. Very useful one of them identifies all the unknown transfer functions, those are the transfer functions of the primary and the secondary paths, through the adaptive processing without using any additional signal for identification.[9,10] This particular method, however, will not always provide the proper modeling results, and the conditions for optimizing the modeling results have not been discussed yet. Hence, we must clarify the conditions to improve the on-line modeling method. It will provide the great possibility to build up the active noise control systems with better performance.

In this paper, we carefully investigate the conditions for optimal on-line modeling through theoretical approach and computer simulation. Theoretical analysis will contribute the particular conditions for accurate on-line modeling that relating to the noise control adaptive filter. The theoretical results are confirmed through the computer simulation in which the impulse responses measured in a vehicle cabin are used.

2. LIMITATION OF FILTERED-X LMS ADAPTIVE FILTER

2.1 Active Noise Control System

A block diagram of the active noise control (ANC) system that uses the filtered-x LMS algorithm is shown in Fig. 1.

In Fig. 1, $x(n)$ is a reference signal at time n and $y(n)$ is an output signal of the noise control adaptive filter. The output signal $y(n)$ is calculated by the convolution of the reference signal $x(n)$ with the impulse response of the noise control adaptive filter $\boldsymbol{w}(n)$. And the filtered reference signal represented by $u_M(n)$ is calculated by the convolution of the reference signal $x(n)$ with an impulse response of the model of the secondary path $\boldsymbol{c}_M$. An impulse response vector of the primary path is represented by $\boldsymbol{h}$, and $d_h(n)$ is the noise at the control point. A vector $\boldsymbol{c}$ means an impulse response of the secondary path, and $d_c(n)$ is the anti-noise at the control point. An error signal is represented by $e(n)$.

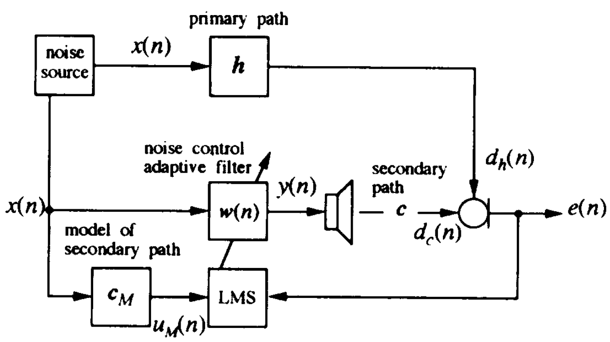

Fig. 1 A block diagram of active noise control system.

We assume that the primary and the secondary paths are finite impulse response (FIR) systems. And the noise control adaptive filter is also FIR type. Using vector form, the tap weight vector update equation for the time domain filtered-x LMS algorithm is given by,

$$\boldsymbol{w}(n+1)=\boldsymbol{w}(n)-\alpha\boldsymbol{u}_M(n)e(n), \qquad (1)$$

where the tap weight vector $\boldsymbol{w}(n)$ and the filtered reference signal vector $\boldsymbol{u}_M(n)$ are T_w-by-1 vectors. The step size (convergence coefficient) α and the error signal $e(n)$ are scalars.

2.2 Influence of Modeling Error

If once the modeling error occurs, for example, when the impulse response of the secondary path is time variant, the filtered reference signal vector $\boldsymbol{u}_M(n)$ in equation (1) will differ from the ideal one $\boldsymbol{u}(n)$ that is calculated by the convolution of the reference signal $x(n)$ with the impulse response of the secondary path $\boldsymbol{c}$. The difference caused by modeling error will lead the noise control adaptive filter into improper adaptation.

In the worst case, the adaptive filter will be unstable.[3-6] On the other hand, if the noise control adaptive filter is stable, the noise reduction performance of ANC system under modeling error condition will be inferior to that under ideal condition to some extent in general.[3,6] Therefore, it is necessary to use the on-line modeling system that identifies the characteristic of the secondary path.

3. ON-LINE MODELING OF PRIMARY AND SECONDARY PATHS

3.1 Conditions for Optimal On-line Modeling

The error signal $e(n)$ is expressed as equation (2).

$$e(n)=d_h(n)+d_c(n). \qquad (2)$$

When the primary and the secondary paths are the finite impulse response systems, the noise $d_h(n)$ and the anti-noise $d_c(n)$ in equation (2) are rewritten as:

$$d_h(n)=\boldsymbol{x}(n)^{\mathrm{T}}\boldsymbol{h}, \qquad (3)$$

and

$$d_c(n)=\boldsymbol{y}(n)^{\mathrm{T}}\boldsymbol{c}, \qquad (4)$$

where the reference signal vector $\boldsymbol{x}(n)$ and the unknown impulse response vector of the primary path $\boldsymbol{h}$ are T_h-by-1 vectors. And the output signal vector of the noise control adaptive filter $\boldsymbol{y}(n)$ and the unknown impulse response vector of the secondary path $\boldsymbol{c}$ are T_c-by-1 vectors. Superscript T expresses the transpose of matrix.

Applying the equation (3) and (4) into the equation (2), the error signal $e(n)$ is expressed as:

$$e(n)=[\boldsymbol{x}(n)^{\mathrm{T}} \quad \boldsymbol{y}(n)^{\mathrm{T}}]\begin{bmatrix} \boldsymbol{h} \\ \boldsymbol{c} \end{bmatrix}. \qquad (5)$$

Therefore, the unknown vectors $\boldsymbol{h}$ and $\boldsymbol{c}$ will satisfy the equation (6).

$$\mathrm{E}\begin{bmatrix} \boldsymbol{x}(n)\boldsymbol{x}(n)^{\mathrm{T}} & \boldsymbol{x}(n)\boldsymbol{y}(n)^{\mathrm{T}} \\ \boldsymbol{y}(n)\boldsymbol{x}(n)^{\mathrm{T}} & \boldsymbol{y}(n)\boldsymbol{y}(n)^{\mathrm{T}} \end{bmatrix}\begin{bmatrix} \boldsymbol{h} \\ \boldsymbol{c} \end{bmatrix}=\mathrm{E}\begin{bmatrix} \boldsymbol{x}(n)e(n) \\ \boldsymbol{y}(n)e(n) \end{bmatrix}, \qquad (6)$$

where E[·] shows the expectation operator. We can identify the unknown vectors $\boldsymbol{h}$ and $\boldsymbol{c}$ correctly by solving the equation (6) when the correlation matrix in the left side is nonsingular.

Now, we represent the correlation matrix in the left side of the equation (6) as $\boldsymbol{R}$. That is,

$$\boldsymbol{R}=\mathrm{E}\begin{bmatrix} \boldsymbol{x}(n)\boldsymbol{x}(n)^{\mathrm{T}} & \boldsymbol{x}(n)\boldsymbol{y}(n)^{\mathrm{T}} \\ \boldsymbol{y}(n)\boldsymbol{x}(n)^{\mathrm{T}} & \boldsymbol{y}(n)\boldsymbol{y}(n)^{\mathrm{T}} \end{bmatrix}.$$

The size of the matrix $\boldsymbol{R}$ is (T_h+T_c)-by-(T_h+T_c), and consequently, the matrix $\boldsymbol{R}$ is nonsingular when its rank is T_h+T_c. It is not always ensured, however, that the nonsingularity of the correlation matrix $\boldsymbol{R}$ is maintained. When the correlation matrix $\boldsymbol{R}$ is singular, we cannot identify the unknown vectors $\boldsymbol{h}$ and $\boldsymbol{c}$ correctly.

Here, let us discuss the nonsingularity of the matrix $\boldsymbol{R}$ in detail. Using the assumption of statistical independence between the quantities,[4,5,11] the correlation matrix $\boldsymbol{R}$ can be expressed as equation (7).

$$\begin{aligned} &\mathrm{E}\begin{bmatrix} \boldsymbol{x}(n)\boldsymbol{x}(n)^{\mathrm{T}} & \boldsymbol{x}(n)\boldsymbol{y}(n)^{\mathrm{T}} \\ \boldsymbol{y}(n)\boldsymbol{x}(n)^{\mathrm{T}} & \boldsymbol{y}(n)\boldsymbol{y}(n)^{\mathrm{T}} \end{bmatrix} \\ &\quad=\mathrm{E}\begin{bmatrix} \boldsymbol{I_P}^{\mathrm{T}} \\ \boldsymbol{W_P}(n)^{\mathrm{T}} \end{bmatrix}\mathrm{E}[\boldsymbol{x_L}(n) \quad \boldsymbol{x_L}(n)^{\mathrm{T}}] \\ &\quad\cdot\mathrm{E}[\boldsymbol{I_P} \quad \boldsymbol{W_P}(n)], \end{aligned} \qquad (7)$$

where

$$\boldsymbol{x}(n)=\boldsymbol{I_P}^{\mathrm{T}}\boldsymbol{x_L}(n), \quad \boldsymbol{x}(n)^{\mathrm{T}}=\boldsymbol{x_L}(n)^{\mathrm{T}}\boldsymbol{I_P},$$

and

$$\boldsymbol{y}(n)=\boldsymbol{W_P}(n)^{\mathrm{T}}\boldsymbol{x_L}(n), \quad \boldsymbol{y}(n)^{\mathrm{T}}=\boldsymbol{x_L}(n)^{\mathrm{T}}\boldsymbol{W_P}(n).$$

In addition, the size of $\boldsymbol{x_L}(n)$, $\boldsymbol{I_P}$ or $\boldsymbol{W_P}(n)$ is dependent upon T_h, T_w and T_c.

〈CASE 1〉

When the condition $T_h<T_w+T_c-1$ is satisfied, the size of the new reference signal vector $\boldsymbol{x_L}(n)$ is (T_w+T_c-1)-by-1, and $\boldsymbol{I_P}$ is a (T_w+T_c-1)-by-T_h matrix that is written as:

$$\boldsymbol{I_P}=\begin{bmatrix} \boldsymbol{I} \\ \boldsymbol{0}_h \end{bmatrix},$$

where $\boldsymbol{I}$ is a T_h-by-T_h identity matrix and $\boldsymbol{0}_h$ means a $\{(T_w+T_c-1)-T_h\}$-by-T_h zero matrix. The size of the matrix $\boldsymbol{W_P}(n)$ is (T_w+T_c-1)-by-T_c, and the matrix $\boldsymbol{W_P}(n)$ is written as:

$$\boldsymbol{W_P}(n)=\boldsymbol{W}(n),$$

where

$$\boldsymbol{W}(n)=\begin{bmatrix} w(0,n) & 0 & \cdots & 0 \\ w(1,n) & w(0,n-1) & \cdots & \cdot \\ \cdot & w(1,n-1) & \cdots & \cdot \\ \cdot & \cdot & \cdots & \cdot \\ w(T_w-1,n) & \cdot & \cdots & 0 \\ 0 & w(T_w-1,n-1) & \cdots & w(0,n-T_c+1) \\ \cdot & \cdot & \cdots & w(1,n-T_c+1) \\ \cdot & \cdot & \cdots & \cdot \\ \cdot & \cdot & \cdots & \cdot \\ 0 & \cdot & \cdots 0 & w(T_w-1,n-T_c+1) \end{bmatrix}.$$

Thus, the matrix $\mathrm{E}[\boldsymbol{I_P} \quad \boldsymbol{W_P}(n)]$ is expressed as:

$$\mathrm{E}[\boldsymbol{I_P} \quad \boldsymbol{W_P}(n)]=\mathrm{E}\begin{bmatrix} \boldsymbol{I} & \boldsymbol{W}(n) \\ \boldsymbol{0}_h & \end{bmatrix},$$

and the size of $\mathrm{E}[\boldsymbol{I_P} \quad \boldsymbol{W_P}(n)]$ is (T_w+T_c-1)-by-(T_h+T_c).

〈CASE 2〉

When the condition $T_w+T_c-1=T_h$ is satisfied, the size of the vector $\boldsymbol{x_L}(n)$ is T_h-by-1, and $\boldsymbol{I_P}$ is a T_h-by-T_h identity matrix $\boldsymbol{I}$. The size of the matrix $\boldsymbol{W_P}(n)$ is identical to the T_h-by-T_c, and the matrix $\boldsymbol{W_P}(n)$ is written as:

$$\boldsymbol{W_P}(n)=\boldsymbol{W}(n).$$

Thus, the matrix $\mathrm{E}[\boldsymbol{I_P} \quad \boldsymbol{W_P}(n)]$ is expressed as:

$$\mathrm{E}[\boldsymbol{I_P} \quad \boldsymbol{W_P}(n)]=\mathrm{E}[\boldsymbol{I} \quad \boldsymbol{W}(n)],$$

and the size of the matrix $\mathrm{E}[\boldsymbol{I_P} \quad \boldsymbol{W_P}(n)]$ is T_h-by-(T_h+T_c).

⟨CASE 3⟩

When the condition $T_w+T_c-1<T_h$ is satisfied, the size of the vector $\boldsymbol{x}_L(n)$ is T_h-by-1 and $\boldsymbol{I}_P$ is a T_h-by-T_h identity matrix $\boldsymbol{I}$. The size of the matrix $\boldsymbol{W}_P(n)$ is a T_h-by-T_c and the matrix $\boldsymbol{W}_P(n)$ is written as:

$$\boldsymbol{W}_P(n)=\begin{bmatrix} \boldsymbol{W}(n) \\ \boldsymbol{0}_c \end{bmatrix},$$

where $\boldsymbol{W}(n)$ is a (T_w+T_c-1)-by-T_c matrix and $\boldsymbol{0}_c$ means a $\{T_h-(T_w+T_c-1)\}$-by-T_c zero matrix. Thus, the matrix $\mathrm{E}[\boldsymbol{I}_P \quad \boldsymbol{W}_P(n)]$ is expressed as:

$$\mathrm{E}[\boldsymbol{I}_P \quad \boldsymbol{W}_P(n)]=\mathrm{E}\begin{bmatrix} \boldsymbol{I} & \begin{matrix} \boldsymbol{W}(n) \\ \boldsymbol{0}_c \end{matrix} \end{bmatrix},$$

and the size of $\mathrm{E}[\boldsymbol{I}_P \quad \boldsymbol{W}_P(n)]$ is T_h-by-(T_h+T_c).

Next, we discuss the decomposition of the auto-correlation matrix of the reference signal $\mathrm{E}[\boldsymbol{x}_L(n)\ \boldsymbol{x}_L(n)^{\mathrm{T}}]$. Since an auto-correlation matrix is always nonnegative definite and almost always positive definite, we assume here that the auto-correlation matrix $\mathrm{E}[\boldsymbol{x}_L(n) \quad \boldsymbol{x}_L(n)^{\mathrm{T}}]$ in equation (7) is nonsingular. When the matrix $\mathrm{E}[\boldsymbol{x}_L(n) \quad \boldsymbol{x}_L(n)^{\mathrm{T}}]$ is nonsingular, we can decompose it as equation (8) by using Cholesky factorization[11] because the auto-correlation matrix is always symmetric.

$$\mathrm{E}[\boldsymbol{x}_L(n) \quad \boldsymbol{x}_L(n)^{\mathrm{T}}]=\boldsymbol{A}\boldsymbol{A}^{\mathrm{T}}. \tag{8}$$

Accordingly, the correlation matrix $\boldsymbol{R}$ is rewritten as equation (9).

$$\begin{aligned}\mathrm{E}&\begin{bmatrix} \boldsymbol{x}(n)\boldsymbol{x}(n)^{\mathrm{T}} & \boldsymbol{x}(n)\boldsymbol{y}(n)^{\mathrm{T}} \\ \boldsymbol{y}(n)\boldsymbol{x}(n)^{\mathrm{T}} & \boldsymbol{y}(n)\boldsymbol{y}(n)^{\mathrm{T}} \end{bmatrix} \\ &=\mathrm{E}\begin{bmatrix} \boldsymbol{I}_P{}^{\mathrm{T}} \\ \boldsymbol{W}_P(n)^{\mathrm{T}} \end{bmatrix}\boldsymbol{A}\boldsymbol{A}^{\mathrm{T}}\mathrm{E}[\boldsymbol{I}_P \quad \boldsymbol{W}_P(n)].\end{aligned} \tag{9}$$

Equation (9) indicates that the correlation matrix $\boldsymbol{R}$ is represented as the product of the two transpose matrices of each other. Therefore, the rank of the matrix in the right side of the equation (9) is identical to that of the matrix $\boldsymbol{A}^{\mathrm{T}}\mathrm{E}[\boldsymbol{I}_P \quad \boldsymbol{W}_P(n)]$. And the rank of the matrix $\boldsymbol{A}^{\mathrm{T}}\mathrm{E}[\boldsymbol{I}_P \quad \boldsymbol{W}_P(n)]$ is equal to that of the matrix $\mathrm{E}[\boldsymbol{I}_P \quad \boldsymbol{W}_P(n)]$ since the triangular matrix $\boldsymbol{A}$ in equation (9) is nonsingular when the auto-correlation matrix $\mathrm{E}[\boldsymbol{x}_L(n) \quad \boldsymbol{x}_L(n)^{\mathrm{T}}]$ is nonsingular. Thus, we can evaluate the nonsingularity of the correlation matrix $\boldsymbol{R}$ according to the rank of the matrix $\mathrm{E}[\boldsymbol{I}_P \quad \boldsymbol{W}_P(n)]$. If the rank of the matrix $\mathrm{E}[\boldsymbol{I}_P \quad \boldsymbol{W}_P(n)]$ is equal to T_h+T_c, the correlation matrix $\boldsymbol{R}$ is nonsingular.

Since the size of the matrix $\mathrm{E}[\boldsymbol{I}_P \quad \boldsymbol{W}_P(n)]$ in case 2 or case 3 is T_h-by-(T_h+T_c), the rank of $\mathrm{E}[\boldsymbol{I}_P \quad \boldsymbol{W}_P(n)]$ will be always smaller than T_h+T_c. Therefore, we can not identify the unknown impulse response vectors $\boldsymbol{h}$ and $\boldsymbol{c}$ correctly in case 2 or case 3.

On the other hand, the size of the matrix $\mathrm{E}[\boldsymbol{I}_P \quad \boldsymbol{W}_P(n)]$ in case 1 is (T_w+T_c-1)-by-(T_h+T_c). Therefore, the rank of $\mathrm{E}[\boldsymbol{I}_P \quad \boldsymbol{W}_P(n)]$ in case 1 is T_h+T_c if the tap length of the noise control adaptive filter T_w is longer than the tap length of the primary path T_h, and one of the tap weights $\mathrm{E}[w(T_h)]\sim\mathrm{E}[w(T_w-1)]$ is a non-zero coefficient at least when the tap weight vector of the noise control adaptive filter is represented as equation (10).

$$\begin{aligned}\mathrm{E}[\boldsymbol{w}(n)]=\mathrm{E}[&w(0, n)w(1, n) \cdots w(T_h, n) \\ &\cdots w(T_w-1, n)].\end{aligned} \tag{10}$$

As long as the tap weights of the noise control adaptive filter $\boldsymbol{w}(n)$ satisfy the above conditions, we can expect the accurate on-line modeling.

However, it is not always ensured that the above conditions are maintained. If the conditions described above are not satisfied, we may manipulate the tap weights to meet the requirement with the risk of degradation of the noise reduction performance.

3.2 On-line Adaptive Modeling

When the correlation matrix in the equation (6) is nonsingular, we can identify the unknown vectors $\boldsymbol{h}$ and $\boldsymbol{c}$ correctly by solving the equation (6). Several methods can be applied to solving the equation (6), and one of them is the on-line adaptive modeling. A block diagram of the on-line adaptive modeling system is shown in Fig. 2.

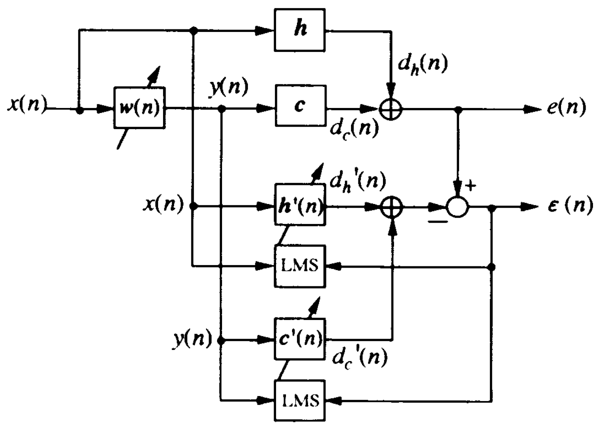

Fig. 2 A block diagram of on-line adaptive modeling system.

In Fig. 2, $\boldsymbol{h}'(n)$ represents the tap weight vector of the adaptive filter that is used to identify the unknown impulse response of the primary path $\boldsymbol{h}$. And $\boldsymbol{c}'(n)$ is the tap weight vector of the adaptive filter that is used to identify the unknown impulse response of the secondary path $\boldsymbol{c}$. The estimated noise or anti-noise at the control point is represented by $d_h'(n)$ or $d_c'(n)$. When we use the LMS algorithm for adaptation, the tap weight vectors of the adaptive filters for identification $\boldsymbol{h}'(n)$ and $\boldsymbol{c}'(n)$ are updated according to the equation (11).

$$\begin{bmatrix} \boldsymbol{h}'(n+1) \\ \boldsymbol{c}'(n+1) \end{bmatrix} = \begin{bmatrix} \boldsymbol{h}'(n) \\ \boldsymbol{c}'(n) \end{bmatrix} + \mu \begin{bmatrix} \boldsymbol{x}(n) \\ \boldsymbol{y}(n) \end{bmatrix} \varepsilon(n), \quad (11)$$

where $\varepsilon(n)$ is the identification error, and μ is the step size.

4. COMPUTER SIMULATION

4.1 Method of Computer Simulation

The computer simulation has been performed to confirm the theoretical results described in the previous section 3.1. A block diagram of the ANC system that was used in our computer simulation is shown in Fig. 3.

In our simulation, the impulse responses acquired in a vehicle cabin were used for the primary and the secondary paths. Because an active noise control system for the interior car noise is one of the typical applications.[12,13] The tap length of those impulse responses were 128, and they were identified by using an adaptive filter with the sampling frequency of 2 kHz. The reference signal $x(n)$ in our computer simulation was white noise with zero mean and the unit power, and the adaptive modeling system shown in Fig. 2 was used for identification.

We used the unique vector in order to confirm the

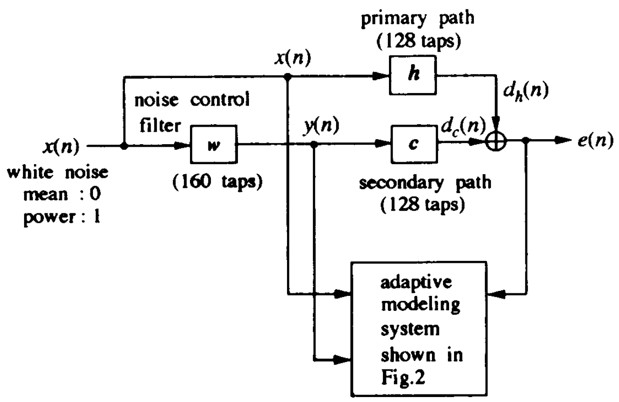

Fig. 3 A block diagram of active noise control system used in computer simulation.

conditions for optimal on-line modeling described in the previous section 3.1. We set the tap weight vector of the noise control adaptive filter $\boldsymbol{w}(n)$ being a constant vector as shown in the equation (12).

$$\boldsymbol{w}(j) = [\delta(1, j)\delta(2, j) \cdots \delta(T_w - 1, j)]. \quad (12)$$

In the equation (12), $\delta(i, j)$ is Kronecker's delta:

$$\delta(i, j) = 1 \quad (i = j)$$
$$= 0 \quad (i \neq j)$$

In other words, only one element of the tap weight vector $\boldsymbol{w}(j)$ is equal to 1 (one) and others are equal to 0 (zero). For exámple, when $T_w = 5$ and $j = 3$, $\boldsymbol{w}(j)$ is written as:

$$\boldsymbol{w}(j) = \boldsymbol{w}(3) = [0 \quad 0 \quad 1 \quad 0 \quad 0]$$

In our simulation, T_w was set as 160.

4.2 Results of Computer Simulation

Figure 4 shows the squared identification errors versus number of iterations. Here, the primary or the secondary path squared identification error was calculated by the below equation:

primary path squared identification error (dB)
$$= 10 \log_{10} \{(d_h(n) - d_h'(n))^2 / \mathrm{E}[d_h(n)^2]\},$$

or

secondary path squared identification error (dB)
$$= 10 \log_{10} \{(d_c(n) - d_c'(n))^2 / \mathrm{E}[d_c(n)^2]\}.$$

The primary or the secondary path squared identification error at $j = 129$ ($> T_h = 128$) is shown in Fig. 4(a) or (b). In this case, both the primary and the secondary path squared identification errors decreased gradually since the tap weights of the noise control filter satisfied the conditions for optimal on-line modeling described in the section 3.1. On the other hand, when the tap weights of the noise control filter did not satisfy the conditions, both of the primary and the secondary paths squared identification errors decreased scarcely. The primary or the secondary path squared identification error at $j = 64$ ($< T_h = 128$) is shown in Fig. 4(c) or (d). In this case, we could not identify the unknown impulse responses correctly.

Identified impulse responses both of the primary and the secondary paths are shown in Fig. 5. Figure 5(c) or (d) shows the identified impulse response of the primary or the secondary path at $j = 129$ ($> T_h = 128$). In this case, all the unknown

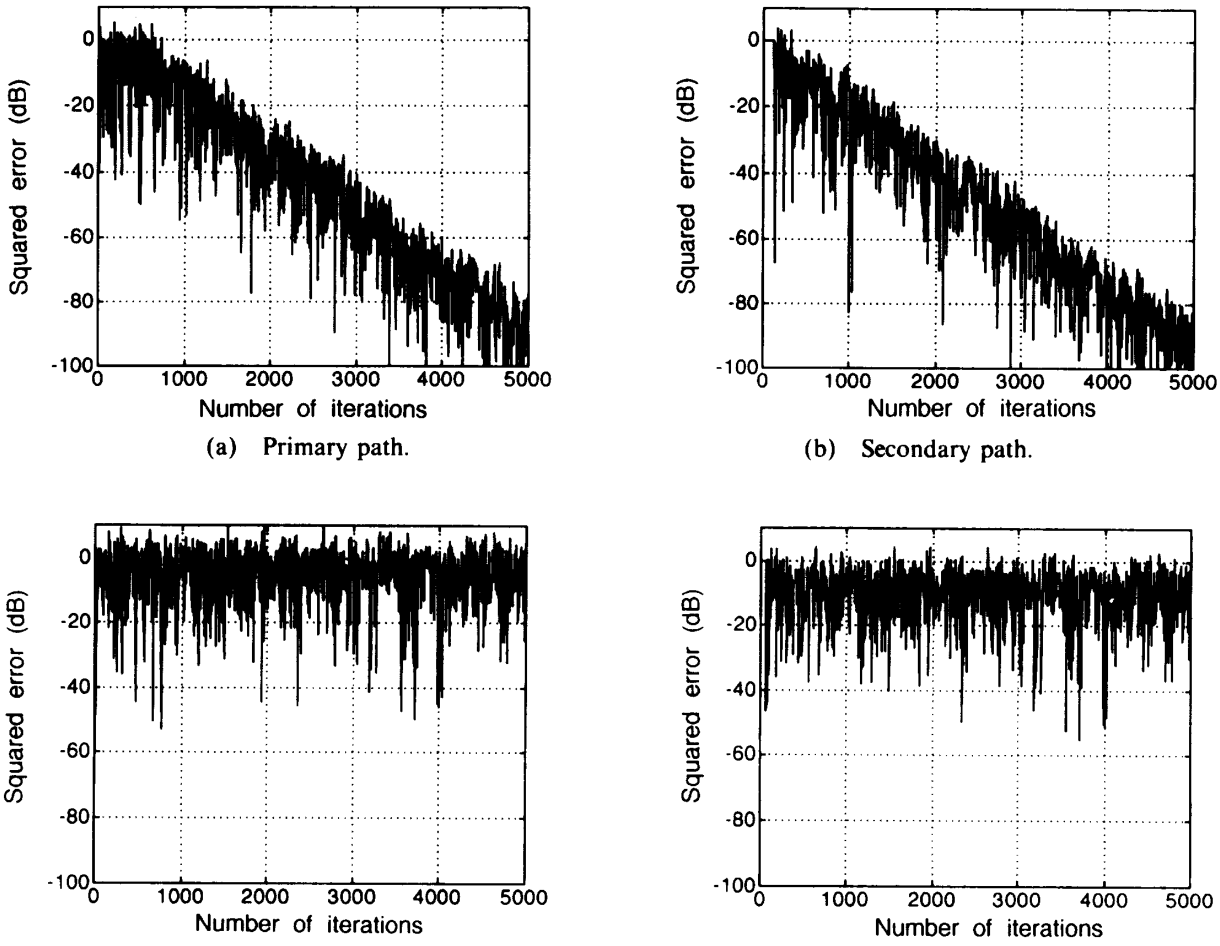

(a) Primary path.

(b) Secondary path.

(c) Primary path.

(d) Secondary path.

Fig. 4 Squared identification errors versus number of iterations. (a), (b) Identification errors when the conditions are satisfied. (c), (d) Identification errors when the conditions are not satisfied.

impulse responses were identified accurately since the conditions for optimal on-line modeling were satisfied. On the other hand, the results of the on-line modeling were different from the true impulse responses when the conditions for optimal on-line modeling were not satisfied. The identified impulse response of the primary or the secondary path at $j=64$ ($<T_h=128$) is shown in Fig. 5(e) or (f). In this case, all the identified impulse responses were not correct.

The mean squared identification errors versus the parameter j in the equation (12) are plotted in Fig. 6. Here, the primary or the secondary path mean squared identification error was calculated by the below equation:

$$\text{primary path mean squared identification error (dB)} = 10 \log_{10} \{E[(d_h(n) - d_h'(n))^2]/E[d_h(n)^2]\},$$

or

$$\text{secondary path mean squared identification error (dB)} = 10 \log_{10} \{E[(d_c(n) - d_c'(n))^2]/E[d_c(n)^2]\}.$$

As soon as the conditions for optimal identification which the tap weights of the noise control filter should satisfy became unsatisfied, the mean squared identification errors increased rapidly.

From these results shown in Figs. 4–6, we can say that it is possible to identify all the unknown impulse responses accurately when the tap weights of the noise control filter satisfy the conditions for optimal on-line modeling. In other words, the results shown in Figs. 4–6 confirm the conditions for optimal on-line modeling derived theoretically in the previous section 3.1.

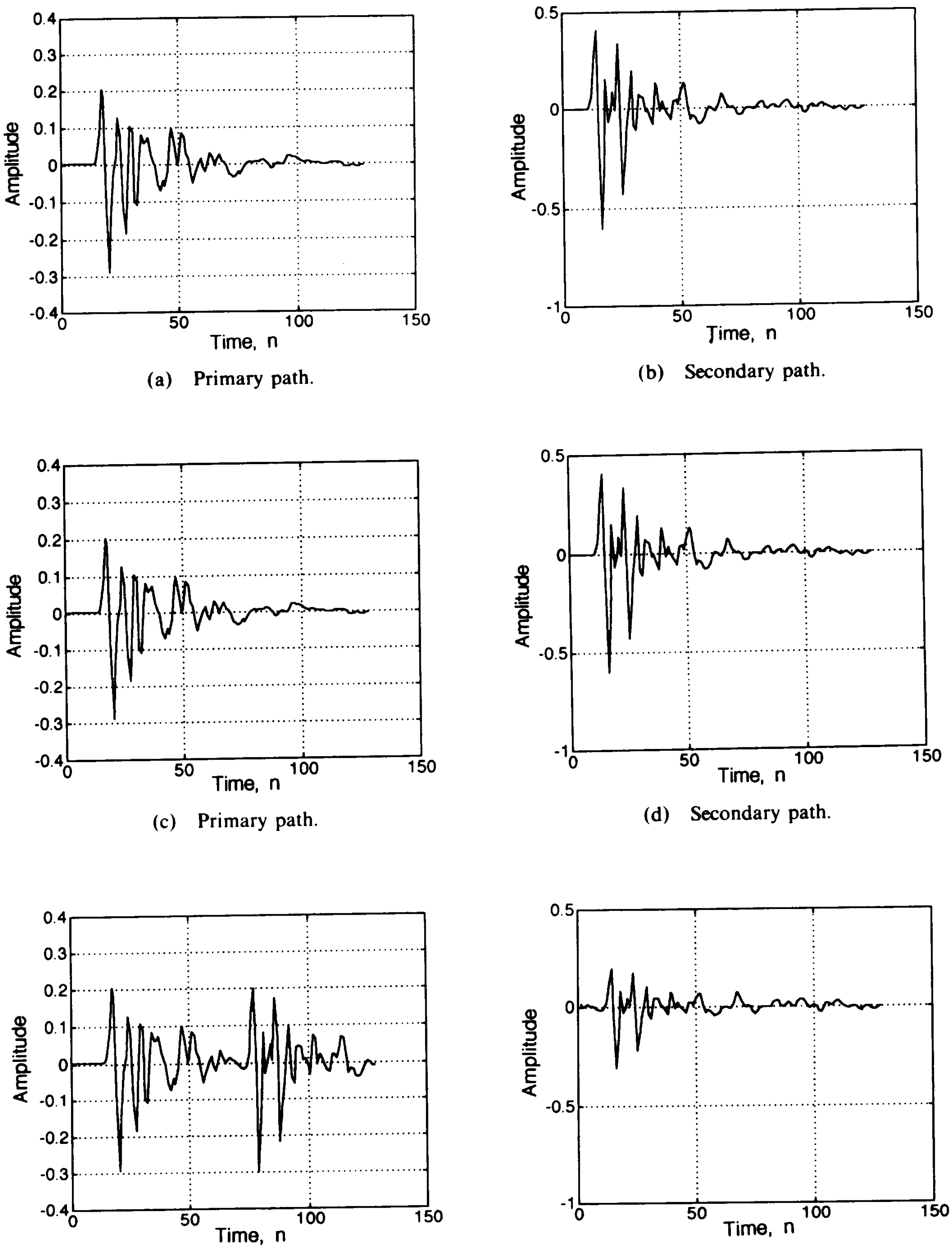

(a) Primary path. (b) Secondary path.

(c) Primary path. (d) Secondary path.

(e) Primary path. (f) Secondary path.

Fig. 5 Identified impulse responses of the primary and the secondary paths. (a), (b) True impulse responses. (c), (d) Identified impulse responses when the conditions are satisfied. (e), (f) Identified impulse responses when the conditions are not satisfied.

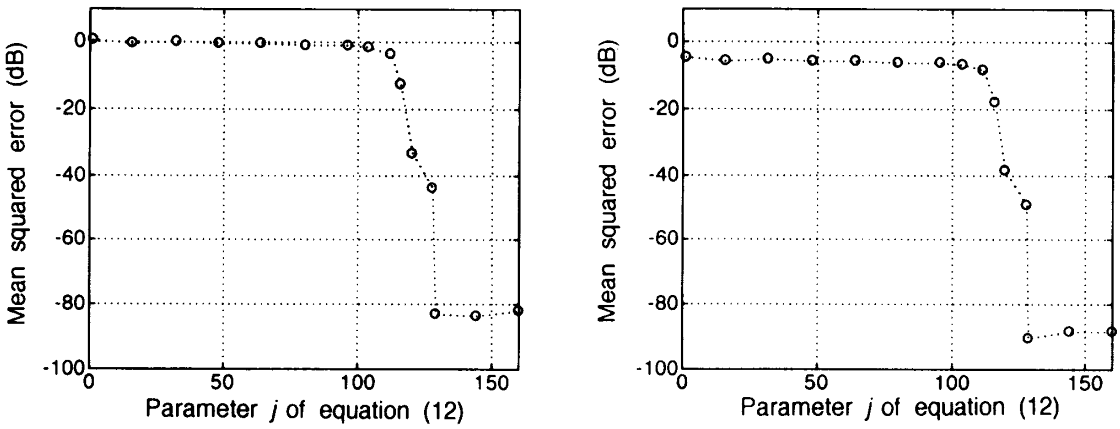

(a) Primary path. (b) Secondary path.

Fig. 6 Mean squared identification error.

5. CONCLUSIONS

In this paper, we investigated the conditions for optimal on-line modeling of the primary and the secondary path characteristics in active noise control systems without using any additional signal for identification. Theoretical analysis produces the specific conditions which the noise control adaptive filter should satisfy. And the theoretical results were confirmed by the computer simulation. In this simulation, the impulse responses acquired in a vehicle cabin were used as the primary and the secondary paths. Thus, we confirmed not only the theoretical results but also derived the useful information for the realization of better interior car noise control systems.

REFERENCES

1) B. Widrow and S. D. Sterns, *Adaptive Signal Processing* (Prentice-Hall, Englewood Cliffs, 1985), pp. 288-294.

2) S. J. Elliott, I. M. Stothers, and P. A. Nelson, "A multiple error LMS algorithm and its application to the active control of sound and vibration," IEEE Trans. Acoust. Speech Signal Process. **ASSP-35**, 1423-1434 (1987).

3) C. C. Baucher, S. J. Elliott, and P. A. Nelson, "The effects of modeling errors on the performance and stability of active noise control system," Proc. Conf. on Recent Advances in Active Control of Sound and Vibration, 290-301 (1991).

4) S. D. Snyder and C. H. Hansen, "The influence of transfer functions and acoustic time delays on the implementation of the LMS algorithm in active noise control systems," J. Sound Vib. **141**, 409-424 (1990).

5) S. D. Snyder and C. H. Hansen, "The effect of transfer function estimation errors on the filtered-x LMS algorithm," IEEE Trans. Signal Process. **SP-42**, 950-953 (1994).

6) N. Saito and T. Sone, "The method to evaluate the system models for the filtered-x LMS adaptive filters," Proc. Inter-Noise 94, 1249-1252 (1994).

7) L. J. Eriksson and M. C. Allie, "Use of random noise for on-line transducer modeling in an adaptive active attenuation system," J. Acoust. Soc. Am. **85**, 797-802 (1989).

8) Sen. M. Kuo and J. Luan, "Multiple-channel error path modeling with the inter-channel decoupling algorithm," Proc. Conf. on Recent Advances in Active Control of Sound and Vibration, 767-777 (1993).

9) D. C. Swanson, "The generalized multichannel filtered-x algorithm," Proc. Conf. on Recent Advances in Active Control of Sound and Vibration, 550-561 (1993).

10) D. C. Swanson, "Frequency-domain implementation of the filtered-x algorithm with on-line system identification," Proc. Conf. on Recent Advances in Active Control of Sound and Vibration, 562-573 (1993).

11) S. Haykin, *Adaptive Filter Theory* (Prentice-Hall, Englewood Cliffs, 1986), pp. 314-316, 221-224.

12) A. M. McDonald, S. J. Elliott, and M. A. Stokes, "Active noise and vibration control within the automobile," Proc. Int. Symp. on Active Control of Sound and Vibration, 147-156 (1991).

13) Y. Kurata and N. Koike, "Adaptive active attenuation of interior car noise," Proc. Int. Symp. on Active Control of Sound and Vibration, 297-302 (1991).

Nozomu Saito was born in Iwaki, Japan on May 13, 1961. He graduated the Department of Electrical Engineering at Hokkaido University, Sapporo, Japan in 1986 and he received M.E. degree from the same university in 1988. In 1990 he joined Alpine Electronics, Inc. He received Dr. (Infor. Sci.) degree from Tohoku University, Sendai, Japan in 1996. His research interests include automatic control, digital signal processing and their applications to sound field control. He is a member of the Acoustical Society of Japan and the INCE of Japan.

Toshio Sone was born on 14 May 1935. A graduate in electrical engineering at Tohoku University, Japan in 1958. Sone did his graduate work at the same university, where he was awarded his Ph.D. in electrical and communication engineering in 1963. He is now a professor of the Research Institute of Electrical Communication, Tohoku University. He has been engaged in researches on psychological acoustics, electroacoustics, room acoustics and noise control over thirty years. From 1993 to 1995 he was President of the Acoustical Society of Japan.

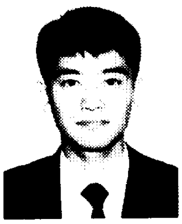

Tomohiko Ise was born in Toyama, Japan on November 11, 1968. A graduate in Information engineering at Tohoku University, Sendai, Japan in 1991. He received the M.E. degree in electrical and communication engineering from the same University in 1993. He joined Alpine Electronics, Inc. in 1993. His research interests include digital signal processing and its applications to sound field control. He is a member of the Acoustical Society of Japan.

Masaichi Akiho graduated the Department of Electrical Engineering at Fukushima National College of Technology in 1979. He is currently a senior engineer at Alpine Electronics, Inc. His research interests are the adaptive sound field control, applications of digital signal processing, and GA. He is a member of the Acoustical Society of Japan.